

UDK: 669.018; 676.056.73537.31

The Influence of Boron addition on Properties of Copper-Zirconium Alloys

M. Simić¹, J. Ružić^{1*}, D. Božić¹, N. Stoimenov², S. Gyoshev²,
D. Karastoyanov², J. Stašić¹

¹Department of Materials, "Vinča" Institute of Nuclear Sciences - National Institute of the Republic of Serbia, University of Belgrade, Belgrade, Serbia

²Institute of Information and Communication Technologies, Bulgarian Academy of Sciences, Sofia, Bulgaria

Abstract:

Copper-zirconium alloys with high conductivity were produced using powder metallurgy. Two-steps manufacturing process, containing mechanical alloying followed by hot pressing, was applied in achieving improved mechanical and physical properties of Cu-Zr alloy. In this paper, the influence of boron on Cu-Zr alloys properties was studied on Cu-1Zr (wt.%) and Cu-1.1Zr-0.3B (wt.%) systems. Scanning electron microscopy, laser nanoparticle sizer, computed tomography and X-ray diffraction were employed for observation of changes in the microstructure during production steps. More specifically – variations in size of the Cu particles, powder mixtures' structural parameters, and development of CuZr phase in binary alloy, CuZr phase and ZrB₂ particles in ternary alloy were observed. It was shown that presence of boron increases dislocation density in ternary alloy over the mechanical alloying time compared to binary alloy. The results presented in this study show higher hardening effect in Cu-Zr-B alloy compared to Cu-Zr alloy, resulting in stable hardness values during thermomechanical treatment. Further, it can be seen that finely dispersed reinforcing ZrB₂ particles in copper matrix does not have significant influence on its conductivity. Moreover, both systems Cu-Zr and Cu-Zr-B exhibit better electrical conductivity after thermomechanical treatment as a result of zirconium reduction in solid solution due to its precipitation.

Keywords: Cu-Zr-B alloy; Mechanical alloying; Hot pressing; Thermomechanical treatment; Conductivity.

1. Introduction

Copper alloys, with their excellent thermal and electrical conductivity, are the first choice for applications in electronics, with the downside of having lower strength. Overcoming this problem has been a subject of many studies aimed at obtaining material resistant to wear action while still retaining high conductivity. As the process of solid-solutionizing has an adverse effect on conductivity, investigations were mainly focused on precipitation and dispersion hardening methods. Copper alloys obtained in similar way [1-4], using mechanical alloying and pressure sintering, showed improved hardness while keeping electrical conductivity. The elements used for copper alloying clearly need to possess high

*) Corresponding author: jovana.ruzic@gmail.com

strength and low specific electrical resistivity. Many of these alloys, however, rely on expensive or hazardous alloying elements such as silver, beryllium or cadmium [5,6].

The Cu-Zr system has shown particularly promising in this context. After aging, dilute Cu-Zr alloys have proven to be mechanically strong with high conductivity at room and elevated temperatures [7,8], which makes them serious candidates for application in certain parts of rocket systems. The alloying content and hence the strength level of Cu-Zr alloys produced by melting and casting processes are, however, restricted by the maximum equilibrium solid solubility of zirconium in copper (≈ 0.2 wt.%). Mechanical alloying and rapid solidification are non-equilibrium procedures providing supersaturated solid solutions of Cu-Zr and therefore increased precipitate amount [9-11]. Using gas atomization as one of the techniques for rapid solidification and hot extrusion, more than 30 years ago significantly more superior mechanical properties in Cu-Zr alloys were obtained compared to the same alloys produced by melting and casting, while maintaining high values of electrical conductivity [7,8]. Superiority regarding mechanical properties was confirmed in later studies in which some other techniques of rapid solidification were applied (melt spinning [9], laser melting [12]). Another way in which the solubility of Zr in copper can be increased is mechanical alloying process. This process, characterized by highly energetic collisions, results in higher solute content which is also more homogeneous. It is also less costly and simpler compared to rapid solidification and is massively used in research and industry [13]. However, compared to some other precipitation hardened copper alloys (Cu-Cr [14], Cu-Ti [15]), Cu-Zr alloys do not precipitation harden to any great extent. The primary benefit of precipitation in this alloy is to refine the grain size and to stabilize the cold-worked structure at elevated temperatures [9]. In order to obtain greater level of hardening in highly-conductive Cu-Zr alloy, a third element is added to this system, most often Cr or B [16].

In this study, Cu-Zr and Cu-Zr-B were fabricated using mechanical alloying for the starting material, while hot pressing was employed as a consolidation method. Aside from the formation of metastable Cu_5Zr , the idea was to promote hardening through ZrB_2 dispersoids in copper matrix, which show slight effect on electrical and thermal conductivity. It was assumed that supplementary beneficial effects could be achieved by adding a third element to this basic system without significant conductivity decreasing. Final aim of this work was to establish the optimum method for obtaining a copper matrix material having the improved hardness and excellent conductivity.

2. Materials and Experimental Procedures

The starting copper, zirconium and boron powders had particle size of ~ 30 μm (99.5% pure), ~ 2 μm (99.5% pure) and ~ 0.08 μm (97% pure), respectively. The Cu-1wt.%Zr and Cu-1.1wt.%Zr-0.3wt.%B mixtures were homogenized for 2 h in Turbula mixer, with the mixture of Cu-1.1wt.%Zr-0.3wt.%B formulated to produce around 2 volume percents of ZrB_2 particles. Homogenization was followed by mechanical alloying (MA) in Netzsch attritor mill with process parameters as: stainless steel balls with 6 mm diameter, ball-to-powder wt. ratio 5:1, inert argon atmosphere, alloying time 1 to 30 h, and stirring speed 330 rpm.

Mechanically alloyed powders were hot pressed at 950°C for 2.5 h, at the pressure of 35 MPa in argon atmosphere. Pressing was conducted in graphite mould. Thermomechanical treatment of the hot pressed samples comprised solution annealing at 950°C for 1 h and water quenching. The degree of plastic deformation was 40 % in all alloys. Hot pressed and thermomechanically treated samples were heat treated at 300, 400, 500, 600, 700, and 800 °C with dwell time of 1 h in hydrogen, and then cooled in water.

Particle size distribution of MA powders as a function of milling duration was investigated by advanced laser nanoparticle sizer Analysette 22 NanoTec plus. Morphology of the mechanically alloyed powders was analyzed by computed tomography (CT) scanning and

scanning electron microscopy (SEM). CT scanning was carried out by Nikon XT H 225 system with reflection head and reconstructed object data was in voxel format (the minimum resolution i.e. voxel size was 3 microns). The powder mixtures and hot pressed samples were characterized by X-ray powder diffraction (XRD) analysis which was performed using Rigaku Ultima IV device with $\text{CuK}\alpha$ Ni filtered radiation. Density of the compacts was determined by Archimedes method in water. Quantitative chemical analysis of the samples was conducted using inductively coupled plasma-atomic emission spectrometry (ICP-AES). This method provided the weight ratio of the elements (Zr, B) contained in master alloys. Vickers macrohardness of hot pressed and thermomechanically treated samples was determined under the load of 1 kg using Buehler Hardness Tester. The microstructure of powders and hot pressed samples was examined with a JEOL-JSM 5800LV scanning electron microscope at an accelerating voltage of 20 kV. Electrical conductivity (σ) was tested on device Forester Sigma Test 2069, at the frequency of 240 kHz, and obtained values are reported as percent of IACS (International Annealed Copper Standard) where $\% \text{IACS} = \sigma \cdot 1.7241 \cdot 10^{-6}$ [17]. Thermal conductivity was calculated based on the Wiedemann–Franz Law [18]: $\sigma \cdot k = T \cdot L$, where k is thermal conductivity ($\text{Wm}^{-1}\text{K}^{-1}$), σ is electrical conductivity (Ωm^{-1}), T is absolute temperature (K), and L is the Lorenz constant ($2.44 \cdot 10^{-8} \text{W}\Omega\text{K}^{-2}$). The presented values for measured quantities – hardness, density and electrical conductivity, were derived from an average of 12 indents, 3 and 5 samples, respectively. Uncertainty values were determined in accordance with the "Guide to expression of uncertainty in measurement" (GUM-ENV 13005).

3. Results and Discussion

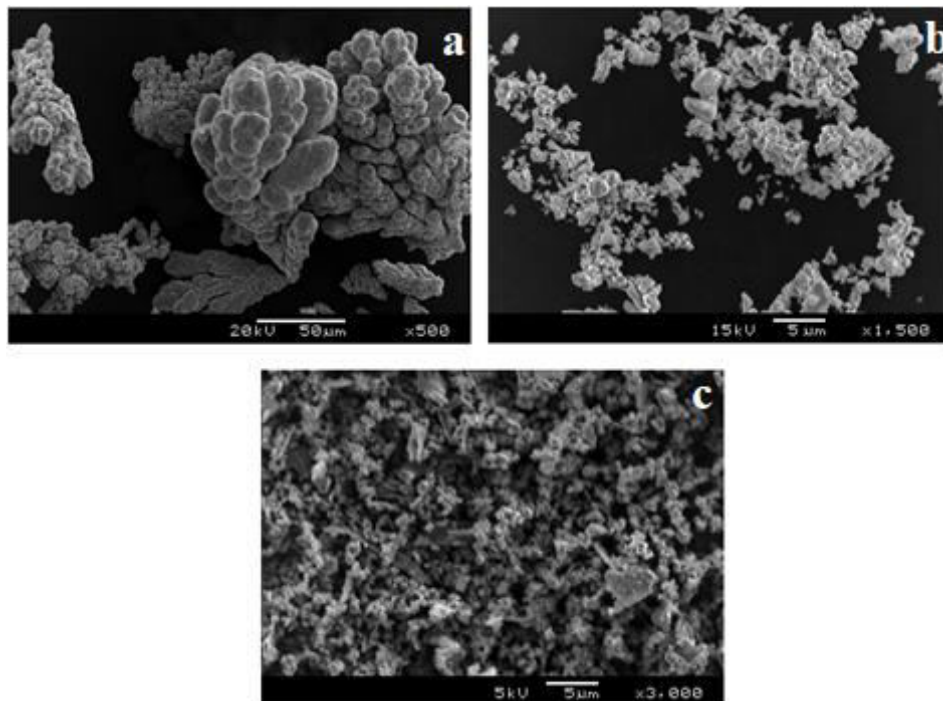


Fig. 1. Microstructure of the starting powders a) copper, b) zirconium and c) boron.

In order to make the mechanical alloying process more efficient, larger particles of the metal matrix (Cu) were chosen compared to the particles of alloying elements, where the average size was approximately 2 μm for Zr (Fig. 1b), and 0.08 μm for B (Fig. 1c). Very

small particles of the starting alloying powders enabled the formation of nano and submicron reinforcement particles in further processes of synthesis. Microphotograph of the starting copper powder particle (Fig. 1a) shows that the copper particles have dendritic shape and their size varies depending on whether they occur as independent branches or as multiple branches with the same base. Zirconium and boron particles (Fig. 1b,c) are irregularly shaped, and being very small they have a tendency of creating “soft” agglomerates with weak interparticle bonds. Based on the given XRD patterns on Fig. 2, it can be concluded that the starting powders do not contain detectable oxides and do not belong to amorphous materials. Patterns of copper and zirconium have clear and sharp peaks of high intensity, while the boron pattern shows lower intensity peaks as a consequence of the present nanoparticles.

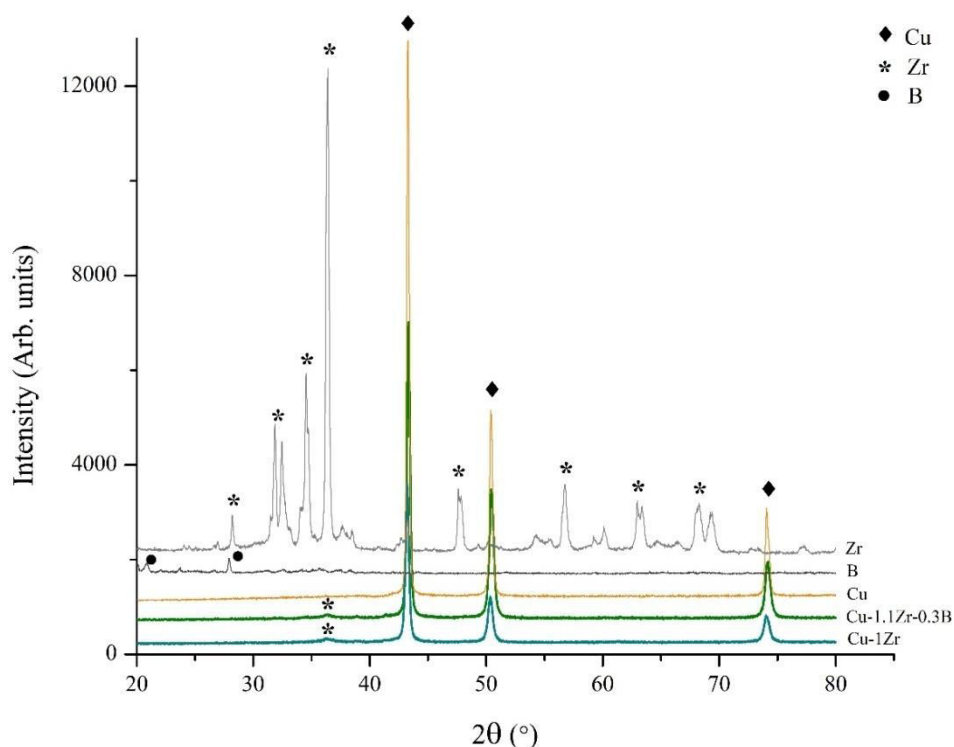


Fig. 2. XRD patterns of the starting powders, Cu-1.1Zr and Cu-1.1Zr-0.3B (wt.%) powder mixture after 25 h milling time.

By using mechanical alloying method and controlling its parameters, it is possible to obtain micro- and nanoscale-structured materials. Milling variables are a type of mill, milling time, temperature, turning velocity, ball-to-powder weight ratio, container atmosphere, process control agent. Among milling parameters, time is an important one which is perfectly controllable, and with optimizing it the best result may be obtained. Structural parameters of the mechanically alloyed powders are calculated from the corresponded X-ray diffractometers using Williamson-Hall analysis [19]. Variations in the structural parameters of Cu-1Zr (wt.%) and Cu-1.1Zr-0.3B (wt.%) powder particles, as a function of mechanical alloying time, are presented in Fig. 3. The results have shown that the optimum milling time would be somewhere in the interval of 25-30 h. Also, X-ray analysis determined that in ternary alloy ZrB₂ reinforcement particles were not formed during milling (Fig. 2).

Plastic deformation of powder particles during milling process leads to increase of the crystal defects and work hardening phenomena in metal matrix due to high energy collisions ball-particle-ball or ball-particle-wall. These processes result in the reduction of average crystallite size in copper particles (Fig. 3a). It is observed that the reduction of crystal size in

ternary alloy is more intensive compared to binary alloy which can be attributed to the effect of hard boron particles. At longer milling times (20 h in ternary, 25 h in binary alloy) and saturation of copper matrix with Zr, or Zr and B atoms, the effects of solute Zr, i.e. Zr and B atoms and work hardening effects may reach a saturated level, and therefore the decreasing trend of average crystallite size slows down and finally stops.

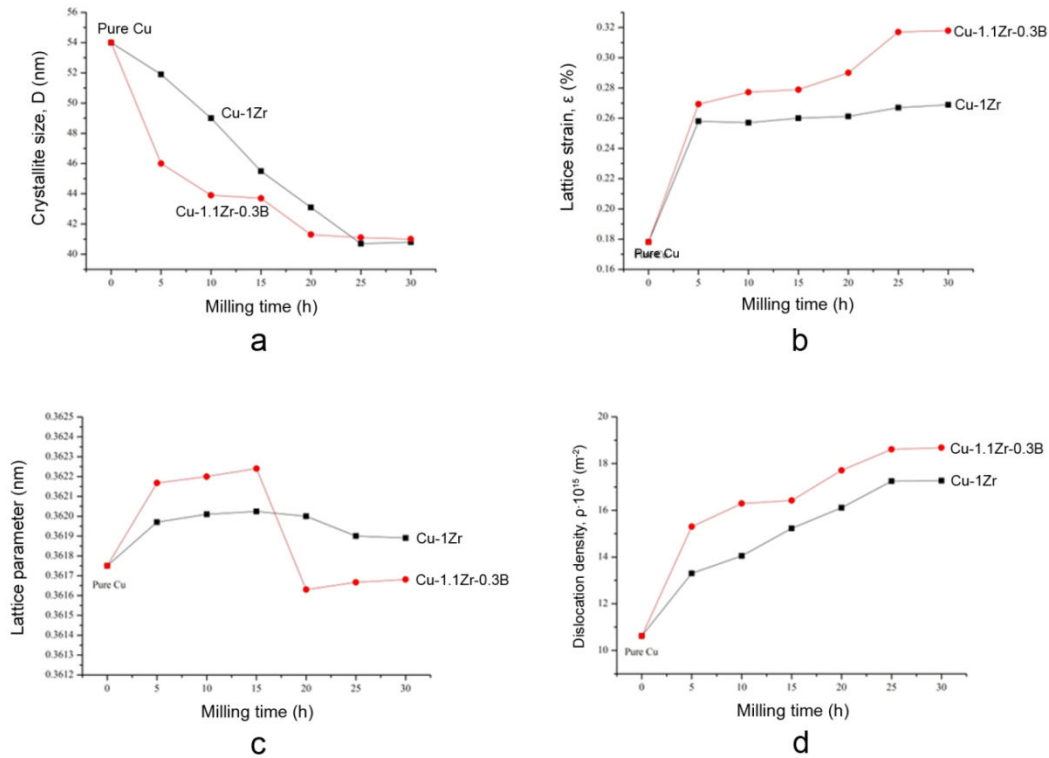


Fig. 3. Structural parameters of MA powder variations versus milling time: a) crystallite size, D (nm), b) lattice strain, ε (%), c) lattice parameter (nm), and d) dislocation density, ρ (m^{-2}).

With the prolonged mechanical alloying time, lattice strain of the unit cell increases in both alloys due to more intensive deformation of crystal lattice, where this incensement is higher in ternary alloy (Fig. 3b). It can be seen that the intensity of the unit cell strain increase is most prominent in the first 5 hours of milling. Lattice parameter in both alloys increases up to 15 h of mechanical alloying (Fig. 3c) which suggests that in this milling time interval solubility of alloying atoms in the copper crystal structure becomes higher. More zirconium particles in the Cu-Zr mixture and more zirconium and boron particles in the Cu-Zr-B mixture lead to steeper concentration gradient of Zr, i.e. Zr and B atoms, in Cu matrix and more diffusion of Zr, i.e. Zr and B atoms, into Cu crystal and its expansion. This is the reason for higher supersaturated solid solution of Zr (Zr and B for ternary system) in Cu matrix with higher Zr content of initial powder mixtures. However, after 15 h of mechanical alloying, lattice parameters are lower in both alloys, and this decrease is much more prominent in ternary alloy. The causes of this lattice parameter drop in of the copper during mechanical alloying can vary. Thus, in Cu-Ti-B ternary alloy, lattice parameter drop is influenced by the formation of Cu_4Ti precipitate [2], while in Cu-Al and Cu-Nb alloys it is the oxidation of the alloying elements [20,21]. In this study, during the mechanical alloying process, neither oxides, nor precipitates, nor borides in ternary alloy were identified (Fig. 2). Lattice parameter is lowered by the formation of recrystallized areas in the structure which are present to a greater extent in ternary alloy. Recrystallization process is a direct consequence of the temperature rise due to ball-particle

collisions during period longer than 15 h of mechanical alloying. This suggests that because of temperature rise, some recovery and recrystallization processes have taken place and at the same time some of the supersaturated dissolved Zr and B atoms have come out of solution leading to a decrease of Cu lattice parameter. It can be observed from Fig. 3d that with the prolonged mechanical alloying time, owing to more intense deformation of particles, multiplication and increased density of dislocations in Cu matrix occurs. Accumulation of dislocations around their obstacles led to the formation of new boundaries and thereof lowering of the crystallite size. Maximum values of dislocation density in both alloys are reached after 25 h of milling, wherein during the whole process of mechanical alloying, this parameter had higher value in ternary compared to binary alloy.

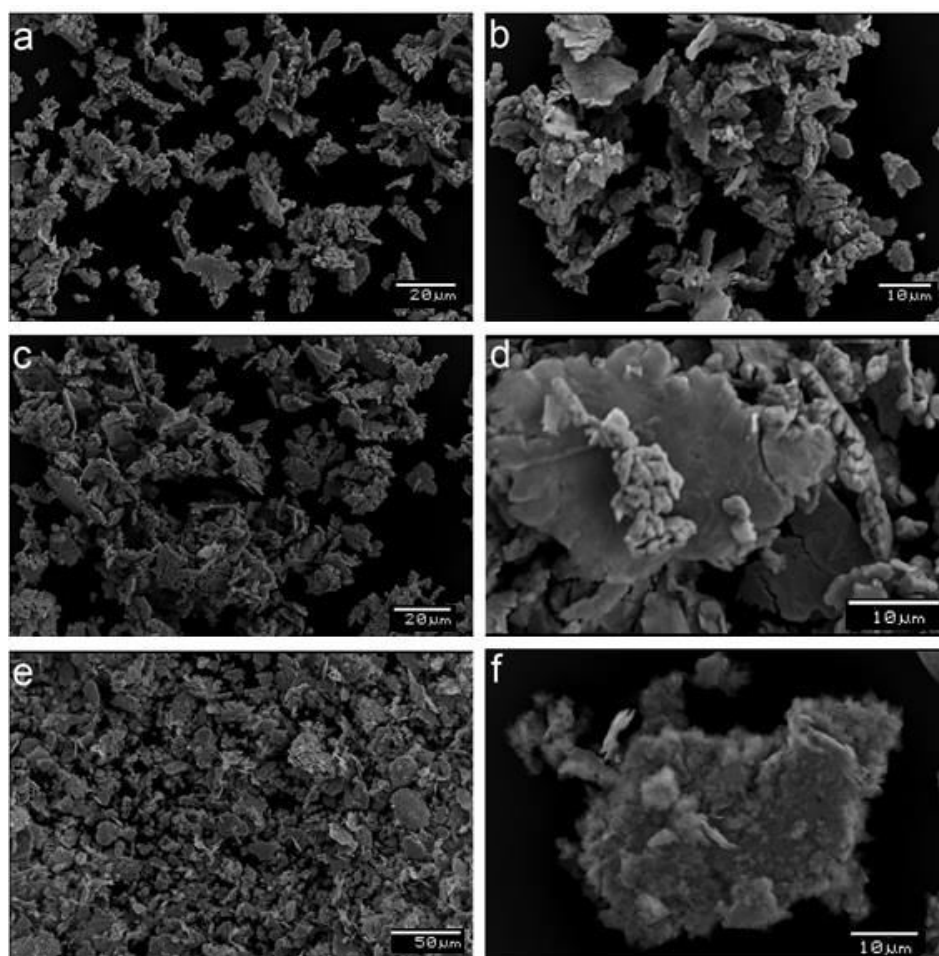


Fig. 4. Shape and size changes of the Cu-1Zr (wt.%) powder particles as a function of mechanical alloying time: a - b: 5 h; c - d: 10 h; e - f: 25 h.

The analysis of morphology of the pure copper particles (Fig. 1a) and mechanically alloyed powders (Fig. 4-7) has shown that the particles in the first hours of mechanical alloying are nonuniform in size and irregularly shaped, while with the prolonged milling their shape becomes more uniform.

It can be observed from the SEM images of the Cu-1Zr (wt.%) system that after shorter milling times (up to 5 h) there were no major changes in binary alloy concerning the morphology of particles compared to starting powders, and most copper particles retained their original shape (Fig. 4a,b). After 10 h of mechanical alloying morphology of particles was mixed: powder contained alloyed, as well as completely non-alloyed copper particles

(Figs. 4c,d). Only after longest milling time, copper particles have lost their original shape (Fig. 4e,f). In certain locations in mechanically alloyed particles, even after 25 h of milling agglomerates formed from the smallest particles of Zr could be observed (Fig. 4f).

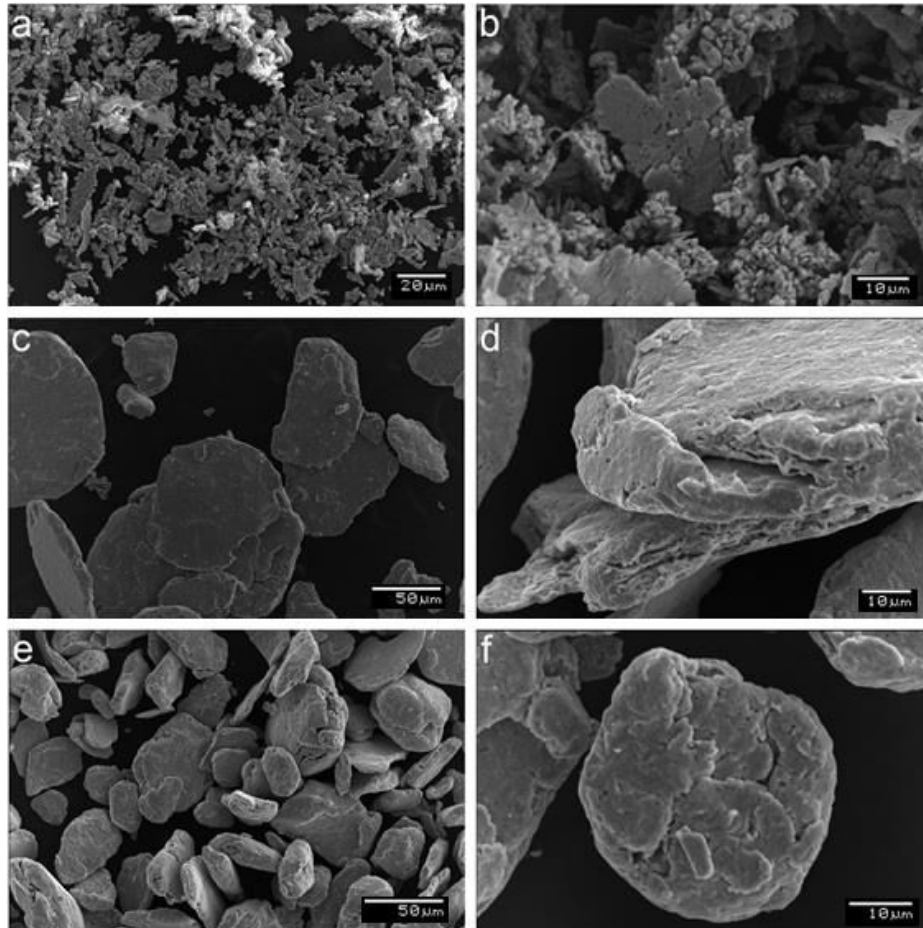


Fig. 5. Shape and size changes of the Cu-1.1Zr-0.3B (wt.%) powder particles as a function of mechanical alloying time: a-b: 5 h; c-d: 10 h; e-f: 25 h.

Unlike powders of binary alloy, changes in the morphology of particles in ternary alloy, Cu-1.1Zr-0.3B (wt.%), could be observed already after shorter milling times (Fig. 5a, b). There were much more newly formed alloyed particles than in Cu-Zr powder, and the present non-alloyed copper particles were increasingly deagglomerated. After 10 h of mechanical alloying, non-alloyed particles of the base metal were not observed in Cu-Zr-B MA powders, and the cold welding processes were more dominant (Fig. 5c, d). This microscopic analysis has helped also to the clarification of the results graphically presented in Fig. 3 which shows that after this milling time, powder particles with boron compared to the ones without boron have smaller crystallite size, more strained crystal lattice, larger lattice parameter (higher solubility of alloying elements) and higher dislocation density. With longer mechanical alloying times all three mechanisms present in this process come to equilibrium: deformation, fracture and cold welding of the particles, which results in a more uniform distribution and shape. After 25 h of treatment in attritor particles take flat, so-called “plate-like” and rounded shape with earlier formation and development of characteristic lamellar structure. Lamellae represent flattened particles of the starting powders which are stuck to each other by cold welding and are a part of one new particle. For longer milling times the

particle distribution of alloying elements has become more uniform (Fig. 5e-f). It is clear that the presence of small, hard particles of boron had a significant role in the fracture process of the copper particles, as well as zirconium particles. To observe 3D view of mechanically alloyed powders the computed tomography was employed. The observed powder mixtures after 30 h of milling time are given in Fig. 6 while changes of the particle size distribution during milling process are displayed in Fig. 7. It can be noticed that after 30 h of milling time in the system Cu-Zr-B there are two fractions of particles, the one with particle size around 7 μm and other with particles size around 50 μm . This phenomenon has not been noticed in Cu-Zr system.

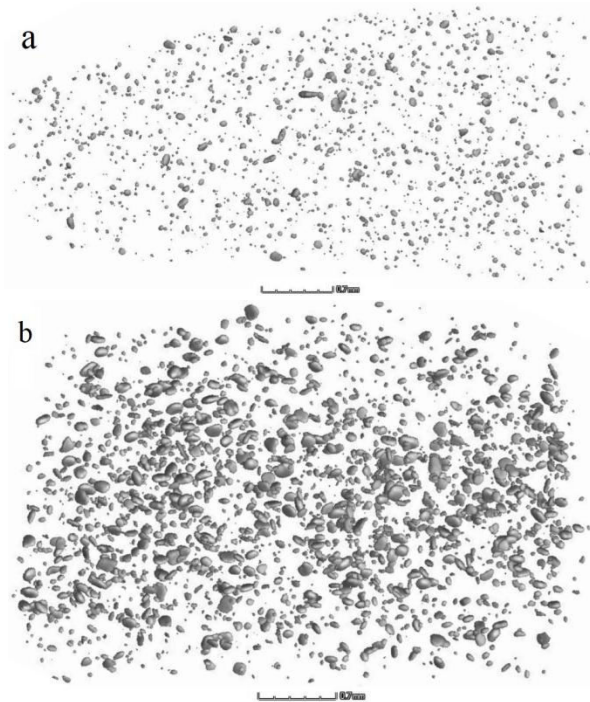


Fig. 6. 3D view of mechanically alloyed powders after 30 h a) Cu-1Zr (wt.%), b) Cu-1.1Zr-0.3B (wt.%) scanned by computed tomography.

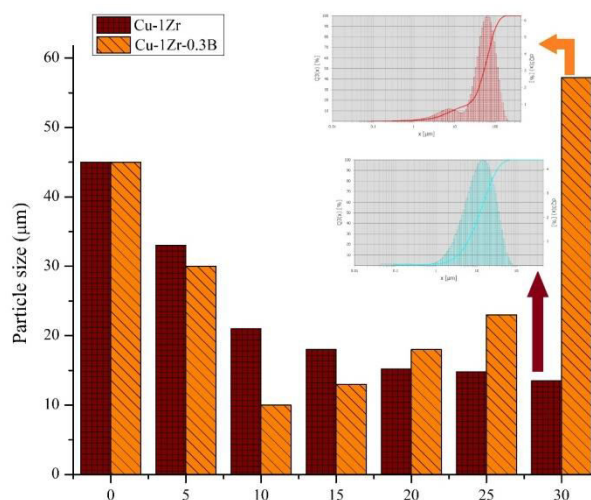


Fig.7. Particle size distribution during milling process.

X-ray diffraction patterns of Cu, Cu-Zr, and Cu-Zr-B samples hot pressed at different temperatures are exhibited at Fig. 8. Identification of ZrB_2 in Cu-1.1Zr-0.3B (wt.%) system is a bit hard using XRD due to the Rigaku Ultima IV device limitation in detection amounts less than 2-3%. ICP analysis showed that amount of ZrB_2 is ~1wt.% (Table I). Thus, ternary system with increased amount of Zr and B are given to illustrate formation of ZrB_2 during hot pressing. It can be seen from Fig. 8 that, except mechanical activation of powders attained with mechanical alloying in attritor, certain thermal energy was necessary for the formation of ZrB_2 particles. Under the constant parameters of hot pressing: $t = 2.5$ h, $p = 35$ MPa, formation of ZrB_2 starts at 650°C and intensifies with further temperature rise. It can be concluded that at 700°C their formation is completely finished since the intensity of peaks on the diffractogram is no different than the ones obtained at the maximum temperature of hot pressing (950°C).

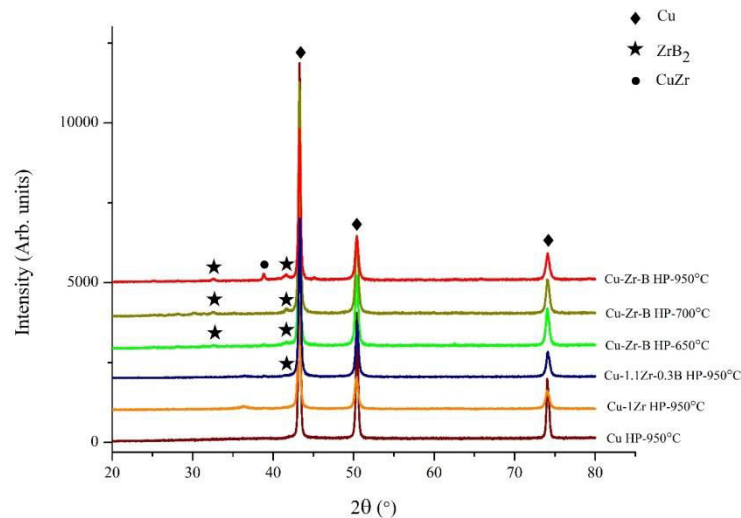


Fig. 8. XRD patterns of the pure Cu, Cu-1Zr, Cu-1.1Zr-0.3B (wt.%) and Cu-4Zr-1B (wt.%) alloy hot pressed at different temperatures.

ICP analysis showed that during mechanical alloying and hot pressing a slight loss in the content of alloying elements occurs compared to the starting powder content, so with the correct choice of parameters for these two processes the chosen ratio of added elements in regards to the starting copper powder is maintained. Insignificant loss in the content of alloying elements is a consequence of smaller number of powder particles left behind on the steel balls and attritor wall in the mechanical alloying process.

Tab. I Chemical analysis of the hot pressed samples.

Powders	Hot-pressed compacts
Cu-1Zr (wt.%)	Cu-0.85Zr (wt.%)
Cu-1.1Zr-0.3B (wt.%)	Cu-0.17Zr-1.1ZrB ₂ (wt.%)

During hot pressing, the densification occurs as a result of powder particles deformation near the surface of their contacts, power law creep and diffusion. Table II indicates that the chosen hot pressing parameters provided alloys with high values of density. Compared to the density of hot pressed pure copper (Fig. 9a), the presence of zirconium and hard ZrB_2 particles in alloys, as well as relatively low pressure of hot pressing, are the reason behind a certain number of pores in the structure (Fig. 9b and c). It could also be observed that in the structure of binary alloy the presence of agglomerated particles (Zr) is higher compared to the ternary alloy structure.

Tab. II Hot pressing parameters of the pure copper and copper alloys.

Metal/Alloys ^a	Temperature [°C]	Time [h]	Pressure [MPa]	Density [g/cm ³]	Open porosity [%]
Cu	900	2	35	8.93	0
Cu-1Zr	950	2.5	35	8.90	2
Cu-1.1Zr-0.3B	950	2.5	35	8.82	2

^acomposition in wt.% of mechanically alloyed powders, before hot pressing

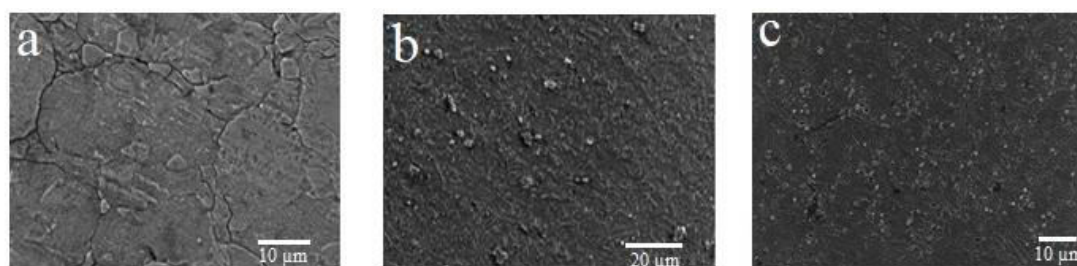


Fig. 9. SEM micrographs showing the microstructure of hot pressed copper and copper alloys: a) Cu, b) Cu-0.85Zr (wt.%), and c) Cu-0.17Zr-1.1ZrB₂ (wt.%).

In the absence of cold work, precipitation of Cu-Zr and Cu-Zr-B alloys is limited, resulting in a very small age hardening effect (Table III). Nevertheless, in comparison with hot-pressed pure copper (589 MPa), hardness values are 1.5 times higher in binary Cu-Zr hot pressed alloy, i.e. nearly two times higher in ternary hot pressed Cu-Zr-B alloy. After thermomechanical regime of hot-pressed samples comprised of solution annealing, quenching, cold working and aging, hardness values of binary and ternary alloys were significantly higher. Hardness increase was influenced by several factors: deformation hardening and precipitation of metastable Cu₅Zr precipitate in binary alloy, i.e. deformation hardening, precipitation of Cu₅Zr precipitate and the presence of ZrB₂ dispersoids formed during hot pressing. Aside from the presence of fine dispersed ZrB₂ particles, higher degree of copper matrix hardening in ternary alloy was also influenced by the absence of large Zr agglomerates characteristic for binary alloy (Fig. 9b). Earlier investigations have shown that cold deformation without solution annealing and quenching produces alloys with significantly lower ductility [10,22]. For this reason, for our further experimental work we used hot-pressed alloys which were solution annealed and quenched prior to deformation.

Tab. III Hardness of Cu-0.85Zr (wt.%) and Cu-0.17Zr-1.1ZrB₂ (wt.%) alloys depending on thermomechanical regime*.

Thermomechanical treatment*	Cu-0.85Zr (wt.%)	Cu-0.17Zr-1.1ZrB ₂ (wt.%)
	Hardness [MPa]	Hardness [MPa]
HP	883	1100
HP+ST+Q+A	706	885
HP+ST+Q+CW+A	1370	1700
HP+CW	1370	1670

*HP – hot pressing: 950°C, 1 h; ST – solution treatment: 980°C, 0.5 h; Q – quenching in water; CW – cold working (40%); A – ageing: 500°C, 1 h.

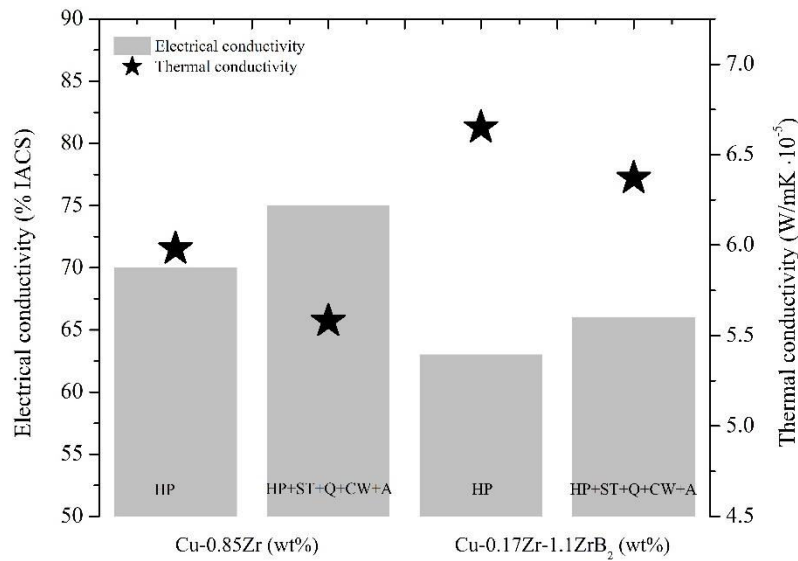


Fig. 10. Electrical and thermal conductivity of Cu-0.85Zr (wt.%) and Cu-0.17Zr-1.1ZrB₂ (wt.%) alloys depending on thermomechanical regime.

Electrical conductivity of the sintered hardened copper alloys can be influenced by multiple factors: size and content of reinforcing particles and their distribution, presence of agglomerates, pores, as well as the appearance of recrystallized grains in the structure [3,22]. In order to lower the negative influence of some factors in determination of electrical properties, samples with the best distribution of alloying elements, i.e. reinforcing particles (25 h of mechanical alloying), minimum pore content (TP: 950°C, 2.5 h, 35 MPa), and without recrystallized grains in the structure (thermomechanical regime: HP+ST+Q+CW+A) were chosen. In Fig. 10 it was shown that Cu-0.85wt.%Zr and Cu-0.17wt.% Zr-1.1wt.%ZrB₂ compacts have better electrical conductivity after thermomechanical treatment as a result of reduction of zirconium in solid solution due to its precipitation. On the other hand, it was expected for the conductivity of ternary alloy to be lower than that of the binary alloy due to the additional presence of finely dispersed ZrB₂ particles content (Fig. 10).

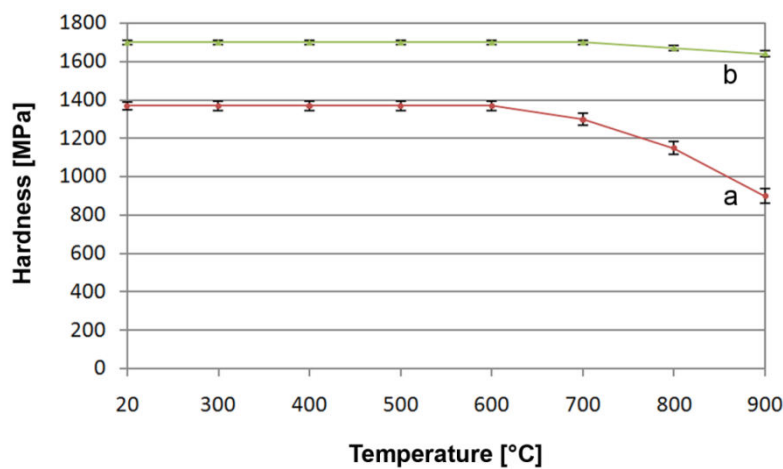


Fig. 11. The effect of annealing temperature (1 h) after thermomechanical treatment (HP+ST+Q+CW) on the hardness of alloys Cu-0.85Zr (wt.%), represents the curve a, and Cu-0.17Zr-1.1ZrB₂ (wt.%), represents curve b.

It was established that the commercial Cu-Zr alloys do not precipitation harden to any great extent. The primary benefit of precipitation in this alloy is to refine the grain size and stabilize the cold-worked structure at elevated temperatures. The effect of annealing temperature after thermomechanical treatment on the hardness of binary Cu-Zr and ternary Cu-Zr-B alloys is shown in Fig. 11.

It is characteristic for binary Cu-Zr alloy that no dramatic hardness decrease is observed after exposure to temperatures up to 600°C which is, in most precipitation hardened copper alloys, usual at temperatures 100 or 200°C lower. This goes in favor to the conclusion that Zr is an excellent candidate for stabilization of the copper structure at increased temperatures which is in agreement with other investigations [23]. Only after annealing at 700°C does the hardness significantly lower due to precipitate coarsening and occurrence of recrystallized grains in structure (Fig. 12a). Compared to the study by Atwater et al. [23], where similar content of Zr was used, in our experiments there was no formation of ZrO₂ particles which, along with the intermetallic Cu₅Zr particles participated in stabilization of the grain size at temperatures above 0.85 T_m for pure copper. Thermal stability of structure up to temperatures this high was achieved in our work only after addition of boron to binary Cu-Zr system, i.e. formation of fine boride particles in the hot pressing process (Fig. 8). ZrB₂ dispersoids prevent grain boundary migration and decrease the rate of grain growth. Only at highest annealing temperature (900 °C) there was a slight decrease of hardness compared to the starting value, as a consequence of a small grain size increase in the structure, and the occurrence of sporadic areas with recrystallized grains (Fig. 12b).

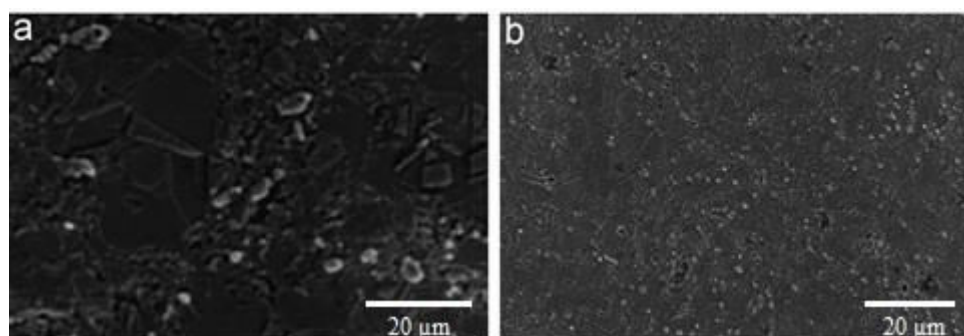


Fig. 12. Microstructure of: a) Cu-0.85Zr (wt.%) alloy after annealing at 700°C, 1 h; b) Cu-0.17Zr-1.1ZrB₂ (wt.%) alloy after annealing at 900°C, 1 h.

We were not able to eliminate the partial presence of larger individual Zr particles, as well as agglomerated Zr and sporadic agglomerated ZrB₂ particles even with the most favorable thermomechanical regime which reflected on somewhat lower values of electrical conductivity and hardness from the expected in the investigated alloys. Regardless of this fact, it can be stated that, compared to some other sintered and hardened copper alloys, we have obtained quite good values of electrical conductivity and hardness (Table IV).

The obtained results are rather optimistic that we are on the right path to obtain a new group of hardened highly-conductive copper alloys, using powder metallurgy techniques, which would find their application not just in electronics but also in nuclear and rocket technology. In the last couple of years, many researchers have been attracted to studies related to optimization of manufacturing processes based on started powders properties, and relations between starting powders and materials' final properties [4,31,32]. Hence, further investigations will primarily be focused on finding the most favorable content of Zr and B in copper matrix and even more optimum thermomechanical processing regimes, in order to achieve the best combination of microstructural, mechanical, physical and technological properties of these alloys.

Tab. IV Hardness and electrical conductivity of various copper alloys obtained through different processes.

Alloy	Process	Hardness [MPa]	Electrical conductivity [% IACS]	Literature
Cu-1at.%Cr	Milling+sintering	1570	48.7	[14]
Cu-0.66wt.%Cr	Melt spinning	1814	80	[24]
Cu-0.5wt.%Cr	ECAP	1716	74.2	[25]
Cu-0.5wt.%Cr	MA+hot pressing	2060	85	[3]
Cu-1at.%Cr-4at.%SiC	Milling+sintering	1765	43	[14]
Cu-3.5wt.%TiB ₂	Melting+drawing	873	64.3	[26]
Cu-10wt.%Cr-3wt.%Ag-5wt.%Al ₂ O ₃	MA+high pressure sintering	4050	25	[27]
Cu-4at.%Cr-2at.%Nb	Milling+hot pressing	2700	57	[28]
Cu-2wt.%Y ₂ O ₃	Milling,sintering+hot deforming	1160	67	[27]
Cu-1.5 wt.%ZrO ₂	Milling,sintering+hot deforming	1345	79	[29]
Cu-1wt.%Al-0.6wt.%Al ₂ O ₃	MA+hot pressing	2350	47	[30]
Cu-0.85wt.%Zr	MA+hot pressing + ST+Q+CW+A	1370	75	This work
Cu-0.17wt.%Zr-1.1wt.%ZrB ₂	MA+hot pressing + ST+Q+CW+A	1700	66	This work

4. Conclusion

The present study leads to following conclusions:

- Two copper-based alloys: precipitation-hardened Cu–0.85wt.%Zr and multiple-hardened Cu–0.17wt.%Zr–1.1wt.%ZrB₂ were prepared by PM techniques - mechanical alloying and hot pressing.
- The microstructure of mechanically alloyed powders consisted of supersaturated solid solution of zirconium in copper for Cu–Zr alloy, i.e. supersaturated solid solutions of zirconium and boron in copper for Cu–Zr–B alloys. Mechanically alloyed powders showed the best distribution of alloying elements in the copper matrix after 25-30 h of milling.
- Nearly theoretical density alloys with homogeneous microstructure were obtained during 150 min of hot pressing at 950°C under the applied pressure of 35 MPa. In Cu–Zr–B alloys *in situ* formation of ZrB₂ occurred only after hot pressing of mechanically alloyed powder in the temperature interval of 650-690°C.
- Maximum hardening of the Cu–0.85wt.%Zr alloy was obtained after 40% cold working and aging at 500 °C due to the influence of precipitation of metastable Cu₅Zr. In case of Cu–0.17wt.%Zr–1.1wt.%ZrB₂ alloy, hardening is a consequence of simultaneous influence of the following factors: cold working, precipitation of metastable Cu₅Zr, and the presence of ZrB₂ particles. Multiple-hardened Cu–

0.17wt.%Zr-1.1wt.%ZrB₂ alloy yields higher hardness values compared to the binary Cu-0.85wt.%Zr alloy, owing to ZrB₂ dispersions formed during hot pressing.

- Binary and ternary copper based alloys were obtained with high thermal and electrical conductivity and these values were, apart from appropriate thermomechanical processes, influenced by the applied content of alloying elements.
- Thermal stability of the structure in ternary copper alloy is more superior compared to binary alloy due to the presence of dispersed fine ZrB₂ particles and the absence of large Zr agglomerates in the copper metal matrix.

Acknowledgments

The work regarding the optimization of the manufacturing processes and particle characterization is financially supported by the European Union's Horizon 2020 research and innovation programme under the Marie Skłodowska-Curie grant agreement No 797372 (DeMoMet project). The data regarding milling parameters is supported by the Bulgarian National Science Fund through project No KP-06-N47/5. The work regarding thermomechanical treatment and sample characterization is funded by the Ministry of Education, Science and Technological Development of the Republic of Serbia (grant agreement No 451-03-47/2023-01/ 200017).

5. References

1. C. Sauer, R. Laag, R. Rein, E. Friedrich, G. Petzow, Proc. powder metallurgy world congress, 6 (1992) 103-113.
2. S. J. Dong, Y. Zhou, Y. W. Shi, B. H. Chang, Metall. Mater. Trans A., 33A (2002) 1275-1280.
3. D. Božić, J. Ružić, J. Stašić, V. Rajković, Int. J. Mater. Res., 105 (2014) 194-199.
4. J. Ružić, M. Simić, N. Stoimenov, D. Božić, J. Stašić, Metall. Mater. Eng., 27 (1), (2021) 1-13.
5. L. Arnberg, U. Backmark, N. Backstrom, J. Lange, Mater. Sci. Eng., 83 (1986) 115-121.
6. M. Krupiński, P. E. Smolarczyk, M. Bonek, Materials. 13 (11) (2020), 2430-2443.
7. M. Azimi, G. H. Akbari, J. Alloy. Comp., 555 (2013) 112-116.
8. Z. C. Zhang, R.C. Wang, C.Q. Peng, Y. Feng, X.F. Wang, X. Wu, Z.Y. Cai, Trans. Nonferrous Met. Soc. China, 31 (12) (2021) 3772-3784
9. Y. Yang, Q. Lei, H.Liu, J. Hong, Z. Han, Q. An, J. Shan, X. Chen, H. Xu, Z. Xiao, S. Gong, Mater. Des., 2019 (2022) 110784-110792.
10. V. K. Sarin, N. J. Grant, Powder Metall. Int., 11 (1979) 153-157.
11. M. Azimi, G. H. Akbari, J. Alloy. Comp. 509 (2011) 27-32.
12. J. Ružić, J. Stašić, V. Rajković, D. Božić, Mater. Des., 62 (2014) 409-415.
13. C. Suryanarayana, Mechanical Alloying and Milling, Marcel Dekker, New York, 2004.
14. P. Sahani, S. Mula, P. K. Roy, P. C. Kang, C.C. Koch, Mater. Sci. Eng. A, 528 (2011) 7781-7789.
15. B.Rouxel, C. Cayron, J. Bornand, P. Sanders, R. E. Logéa, Mater. Des., 213 (2022) 110340-110354.
16. K. S. Kumar, NASA Contr. Rep. 191124, Baltimore, 1993.
17. Copper wire tables, IACS, Circular of the Bureau of Standards No.31 US, 1914.
18. Y. Hu, S. Li, H. Bao, Phys. Rev. B, 103 (10) (2021) 104301- 104312.

19. B. Himabindu, N.S.M.P. Latha Devi, B. Rajini Kanth, Mater. Today: Proc., 47 (2021) 4891-4896.
20. V. Rajković, D. Božić, M. T. Jovanović, Mater. Char., 57 (2006) 94-99.
21. E. Botcharova, M. Heilmaier, J. Freudenberger, G. Drew, D. Kudashov, U. Martin, L. Schultz, J. Alloy. Comp. 351 (2003) 119-125
22. J. S. Andrus, R. G. Gordon, NASA Contr. Rep. 187207, West Palm Beach, 1989.
23. M. A. Atwater, R. O. Scattergood, C. C. Koch, Mater. Sci. Eng. A, 559 (2013) 250-256.
24. L. Ping, K. Buxi, C. Xingguo, H. Jinliang, G. Haicheng, Trans. Nonferrous Met. Soc. China, 9 (1999) 723-726.
25. C. Z. Xu, Q. J. Wang, M. S. Zheng, J. W. Zhu, J. D. Li, M. Q. Huang, Q. M. Jia, Z. Z. Du, Mater. Sci. Eng. A, 459 (2007) 303-308.
26. J. P. Tu, N. Y. Wang, Y. Z. Yang, W. X. Qui, F. Liu, X. B. Zhang, H. M. Lu, M. S. Liu, Mater. Lett., 52 (2002) 448-452.
27. S. Bera, W. Lojksky, I. Manna, Mater. Trans. A, 40A (2009) 3276-3283.
28. K. R. Anderson, J. R. Groza, D. G. Ulmer, Scripta Mater., 37 (1997) 179-185.
29. J. P. Stobrawa, Z. M. Rdzawski, W. Gluchowski, J. Domagola-Dubiel, J. Achiev Mater. Manuf. Eng., 54 (2012) 49-57.
30. V. Rajković, D. Božić, A. Devečerski, M. T. Jovanović, Mater. Char., 67 (2012) 129-137.
31. D. D. Phuong, N. V. Luan, P. V. Trinh, T. B. Trung, Sci. Sinter. 54 (1) (2022) 93-103.
32. M. A. Erden, M. F. Tasliyan, Y. Akgul, Sci. Sinter. 53 (4) (2021) 497-508.

Сажетак: Високо проводне легуре бакра са додатком цирконијума произведене су металургијом праха. У постизању побољшаних механичких и физичких својстава Cu-Zr легуре примењен је двостепени процес производње, који садржи механичко легирање праћено топлим пресовањем. У овом раду проучаван је утицај бора на својства Cu-Zr легура поређењем система Cu-1Zr (теж.%) и Cu-1.1Zr-0.3B (теж.%). Промене у микроструктури током производних корака праћене су помоћу метода: скенирајућа електронска микроскопија, ласерско одређивање величина микро- и наночестица, компјутерска томографија и рендгенска дифракција. Посебно су посматране варијације у величини честица бакра, структурних параметара мешавине праха и развој CuZr фазе у бинарној легури, као и CuZr фазе и ZrB_2 честица у терцијарној легури. Показало се да присуство бора повећава густину дислокација у терцијарној легури током механичког легирања у поређењу са бинарном легуром. Резултати приказани у овој студији показују већи ефекат ојачавања у легури Cu-Zr-B у поређењу са легуром Cu-Zr , што резултира стабилним вредностима тврдоће током термичке обраде. Даље, може се видети да фино дисперговане честице ZrB_2 у матрици бакра показују незнатан утицај на њену проводљивост. Такође, оба система Cu-Zr и Cu-Zr-B показују бољу електричну проводљивост након термичке обраде као резултат редукције цирконијума у чврстом раствору услед његовог таложења.

Кључне речи: Cu-Zr-B легура, Механичко легирање, Топло пресовање, Термичка обрада, Проводљивост.

